

# A novel and facile approach for preparing composite core–shell particles by sequentially initiated grafting polymerization

Qin Wang<sup>a,b</sup>, Lianying Liu<sup>a,b</sup>, Wantai Yang<sup>a,b,\*</sup>

<sup>a</sup> State Key Laboratory of Chemical Resource Engineering, Beijing 100029, PR China

<sup>b</sup> College of Materials Science and Engineering, Beijing University of Chemical Technology, Beijing 100029, PR China

Received 11 March 2007; received in revised form 19 July 2007; accepted 8 August 2007

Available online 14 August 2007

## Abstract

With the commercially available vulcanized acrylonitrile butadiene rubber (NBR) latex as a model, a facile approach for the preparation of composite core–shell particles was developed. As the first step, UV photoreduction followed by cross-linking/coupling reactions with benzophenone (BP) as the photoinitiator and trimethylpropane triacrylate (TMPTA) as the accelerator were carried out in order to attach dormant semi-pinacol groups to the surface of the NBR particles (NBR–SP). The second step, carried out under heating, involved the grafting of styrene (St) which was induced from the particle surface by bond breaking of NBR–SP and propagation towards the center of the particles. The grafting efficiency could be kept at a high level, i.e. approx. 90%, and the grafting yield increased with time (could reach up to 140%). Finally, by adding acrylamide (AM) or *N*-vinyl pyrrolidone (NVP) as a second monomer under heating, a composite core–shell particle could be prepared.

© 2007 Elsevier Ltd. All rights reserved.

**Keywords:** Core–shell polymers; Grafting polymerization; Surface

## 1. Introduction

Recently, the preparation of core–shell structures has become a fast-growing topic in colloid and materials science. Particles with core–shell structures have diverse applications in coatings, impact modification, bio-separation, drug delivery systems, etc. [1–5]. Extensive research has been carried out in order to fabricate functional core–shell particles with a variety of strategies. Generally, a core–shell structure can be achieved by seeded emulsion polymerization [6,7] or by self-assembly of block copolymers with selective solubilities to the solvent [8,9]. Furthermore, it is reported that self-assembly of polymer chains on a core surface [10], layer-by-layer deposition [11] and polymerization of monomer absorbed on a core surface

[12–14] are also effective approaches for obtaining core–shell structures.

An alternative method for achieving well-defined core–shell morphology is to graft polymer brushes through the use of initiators tethered chemically to the particle surface [15–23]. This “grafting from” technique provides an opportunity to achieve stable layers of densely grafted polymers with a variety of compositions and functionalities on the surfaces of micro/nanoparticles such as latexes, gold, silica, etc. [19,24–29].

As a hydrogen-abstractable photoinitiator, benzophenone (BP) has been extensively used in surface photo-grafting polymerizations and the initiation proceeds in three steps. First, BP absorbs a photon and forms an excited singlet state (BPS). Then, it yields a more stable excited triplet state (BPT) through intersystem crossing, and finally, the triplet state BPT interacts with weak C–H bonds on the surface of the organic substrate, giving rise to hydrogen abstraction and leaving a semi-pinacol free radical and a surface alkyl free radical that can initiate a surface grafting polymerization [30–32]. Recent studies have reported on a two-step method, consisting

\* Corresponding author. College of Materials Science and Engineering, Beijing University of Chemical Technology, Beijing 100029, PR China. Tel.: +86 10 6443 2262; fax: +86 10 6441 6338.

E-mail address: [yangwt@mail.buct.edu.cn](mailto:yangwt@mail.buct.edu.cn) (W. Yang).

in the coupling of BP onto the surface of a plane solid organic polymer by the above photoreductions (first step), followed by the initiation of a surface grafting polymerization with some living polymerization character through the cleavage of weak C–C bonds under UV irradiation or heating at a temperature above 80 °C (second step) [33–35].

In the present investigation, we have explored the possibility of utilizing this two-step method for preparing composite core–shell particles with a commercially available vulcanized acrylonitrile butadiene rubber (NBR) emulsion as model latex. No study focuses on the BP coupling two-step method being used for the grafting polymerization on colloidal surface. It is known that the strong scattering of light in an emulsion permits the occurrence of photopolymerization [25,36,37]. Hence, the reaction heterogeneity resulting from the opacity or UV-screening effect of the latex system mentioned above could be minimized. On the other hand, the UV-screening effect of each latex particle could be used in order to limit the grafting reaction to take place only on the surface of the particles. However, the most important scientific issue to address is how to adhere dormant or re-initiating groups onto the surface or subsurface of a particle.

In order to realize this, a novel strategy, depicted in Scheme 1, was proposed. This strategy involved the following steps: (1) BP and the three-functional monomer, trimethylpropane triacrylate (TMPTA), were dissolved in the NBR latex; (2) under UV radiation, a free radical surface/subsurface cross-linking polymerization, that was initiated by the BP photoreduction, would take place due to a UV-screening effect in the latex particles; (3) as a result of the cross-linking

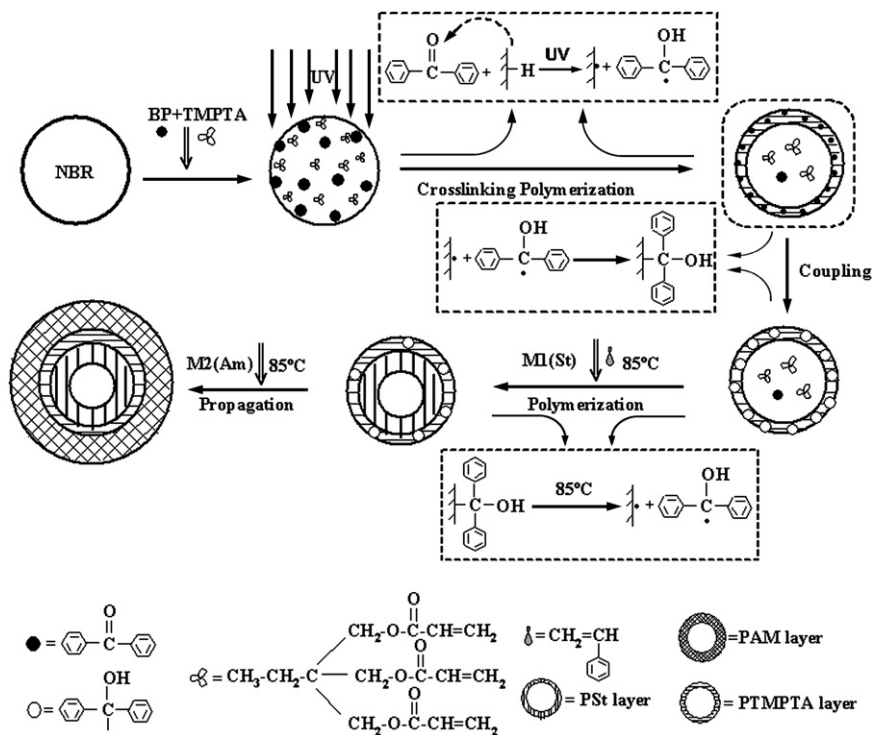
polymerization and the free radical coupling reaction with the semi-pinacol (SP) radicals, particles with large amounts of dormant SP groups would be obtained.

The cross-linking reaction of TMPTA should favor an increase in surface coupling of the SP groups. When the NBR latex carrying surface SP groups contacted with monomers above 80 °C, it was, surprisingly, found that the grafting polymerization did indeed start from the surface of the particles, and then grow inwards to their center for oily monomers such as styrene (St) alternatively grow outwards for hydrophilic monomers such as acrylamide (AM). Moreover, compared with the approaches reported earlier, the advantages of this method for the preparation of composite core–shell particles include a high grafting efficiency (approx. 90%) and a facility in the fabrication process.

## 2. Experimental

### 2.1. Materials

An acrylonitrile butadiene rubber (NBR) latex with a dry rubber content of 50 wt% and a gel content of 80 wt% was generously donated by Lanzhou Chemical Plant. Trimethylpropane triacrylate (TMPTA) was obtained from Tianjin Chemical Reagent Co. and used as received. Styrene (St) and *N*-vinyl pyrrolidone (NVP) were purchased from Beijing Chemical Reagents Company and purified by distillation to remove any inhibitors. Acrylamide (AM) and benzophenone (BP) were obtained from Shanghai Chemical Reagents Co. Ltd., China and used as received.



Scheme 1. The schematic procedure and chemistry for a grafting polymerization on the surface of NBR latex particles. The scheme depicts a generalized mechanism for the grafting reaction.

## 2.2. Synthesis of NBR–SP latex

A mixture of BP (5 g) dissolved in TMPTA (4 g) was added drop-wise into the NBR latex (200 g) under vigorous stirring for at least 1 h. As portrayed in Fig. 1(a), 50 ml of the reaction mixture was placed in a pyrex cylinder (with dimensions 5 cm ( $\Phi$ )  $\times$  9 cm (h)) that was sealed with a thin film of biaxially oriented polypropylene (BOPP) and purged with nitrogen for 30 min. The mixture was then subjected to UV irradiation (with a light intensity of 45 w/m<sup>2</sup> and a 375-W high pressure mercury lamp as a polyspectrum light source emitting light primarily at a wavelength of 365 nm) for 1 h, whilst maintaining a low flow of nitrogen. Stable latex was obtained during the irradiation.

## 2.3. Synthesis of NBR/PSt core–shell particle

Latex (10 g) from the irradiation step, carrying dormant surface SP groups, was diluted with water (35 g), and charged into a 100 ml four-necked round-bottom flask assembled with a mechanical stirrer, thermometer, nitrogen inlet tube and condenser (see Fig. 1(b)). After degassing for 30 min, the flask was placed in a thermostat preheated to 85 °C, and St (5 g) was dripped into it during a period of 15 min. The flask was incubated at 85 °C for 5 h to complete the grafting polymerization on the latex surface.

The obtained NBR/PSt core–shell particles were precipitated in a 2% calcium chloride aqueous solution, washed with hot water at least 5 times, dried at 50 °C for 24 h, placed in a vacuum oven at 50 °C until a constant weight was reached, and finally extracted by Soxhlet with 2-butanone to remove trace amounts of PSt homopolymer.

## 2.4. Synthesis of composite core–shell particles

In a successive step, NBR/PSt core–shell latex (20 g) ( $C_{\text{NBR}} = 7\%$ ,  $C_{\text{St}} = 7\%$ , polymerized at 85 °C for 3 h with a grafting yield of 42%, and a concentration of NBR/PSt core–shell particles of 10%) in a four-necked round-bottom flask was degassed for 30 min and heated to 85 °C. With the introduction of water (12.5 g) and AM (2.5 g) AM or NVP (2.5 g) in an aqueous solution, polymerization was initiated and maintained for 3 h. The end products were extracted by Soxhlet with 2-butanone, followed by water extraction to remove unreacted monomer and homopolymer. As a result, a composite shell composed of PSt and PAM or PVP was constructed.

The monomer conversion ( $C$ ), grafting yield (GY, i.e. the ratio of the weight of grafted polymer to the weight of the NBR particles) and grafting efficiency (GE, i.e. the ratio of the weight of grafted St to the total weight of polymerized St) were calculated according to the following equations:

$$\text{Conversion : } (C, \%) = \frac{W_p}{W_0} \times 100 \quad (1)$$

$$\text{Grafting yield : } (GY, \%) = \frac{W_g}{W_r} \times 100 \quad (2)$$

$$\text{Grafting efficiency : } (GE, \%) = \frac{W_g}{W_p} \times 100 \quad (3)$$

Here,  $W_p$  was the weight of the polymerized St.  $W_0$  was the weight of the St added,  $W_g$  was the weight of the grafted St and  $W_r$  was the weight of the NBR used.

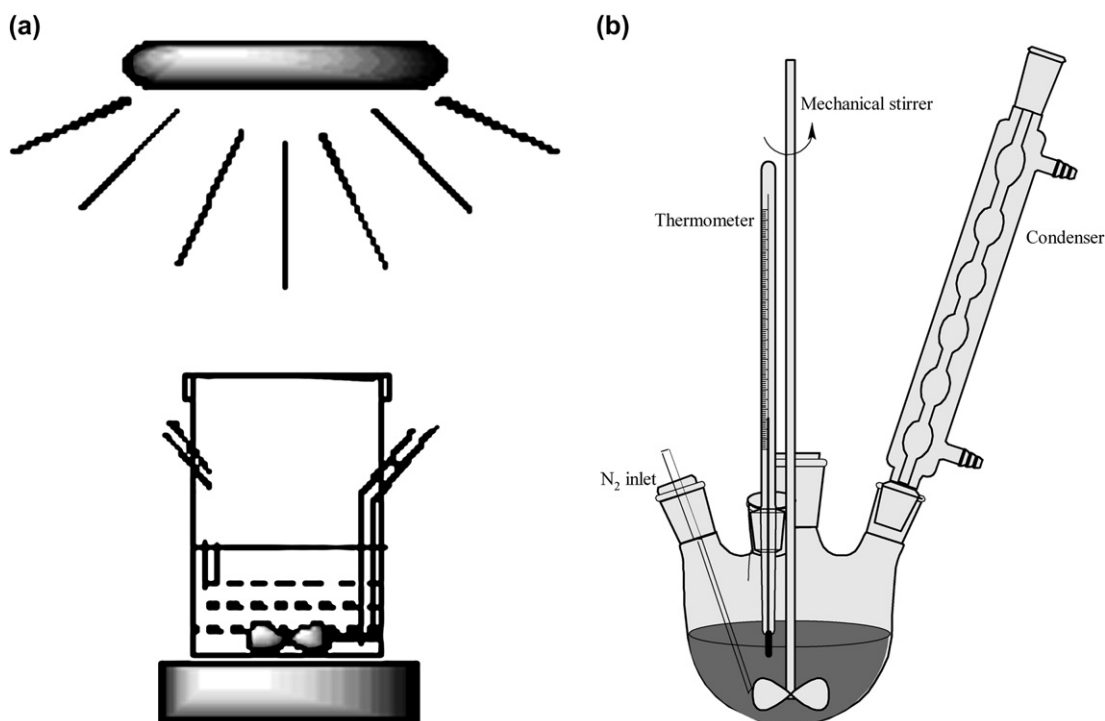


Fig. 1. The experimental setups for (a) the photoreaction and (b) the grafting polymerization.

## 2.5. Characterization

UV–vis spectra were recorded with a CENTRA 20 UV–vis spectrometer over the range of 200–550 nm. Samples for the UV–vis measurements were prepared by casting NBR–SP latex onto PP films. Unreacted BP in the NBR–SP particle was removed by immersion in ethanol for 1 week. FTIR spectra of the samples were obtained using a Nicolet NEXUS 670 spectrometer. The FTIR samples were extracted by Soxhlet with 2-butanone to remove unreacted St and homopolymerized PSt. NMR samples of NBR particles and NBR–SP particles were extracted by Soxhlet with ethanol for 48 h. Solid state NMR  $^{13}\text{C}$  analysis was performed at 75.47 MHz on a Bruker AV-300 spectrometer. The recycle time was 4 s; and 400 scans were required for each experiment. The core–shell structure was visualized by transmission electron microscopy (TEM) (HITACHI H-800) at an acceleration voltage of 200 kV. Samples for TEM observation were stained with 2%  $\text{OsO}_4$  solution in a staining chamber at room temperature for 20 min. The diameters of the latex particles were directly measured by a laser-light scattering spectrometer (Mastersizer 2000) at room temperature after dilution with water.

## 3. Results and discussion

### 3.1. Synthesis of the NBR–SP latex

A low grafting yield (approx. 35% after 10 h) and a low grafting efficiency (approx. 50%) were obtained when using only BP as the photoinitiator when synthesizing the NBR/PSt latex. This indicated that a large amount of homopolymer PSt was produced and a reason behind this could possibly lie in the photoreduction and following coupling reactions of BP and emulsifier or other additives in the commercial NBR latex under UV radiation. In order to resolve this problem, we tested adding TMPTA.

TMPTA is generally used as an accelerator in high energy irradiation cross-linking [38–40]. By transferring radicals in situ, it could significantly increase the irradiation cross-linking efficiency. In our system, the introduction of TMPTA as well as the low energy UV radiation would limit the photoreaction to take place exclusively on the surface of the particles. Thus, two things could be predicted: (1) the cross-linking polymerization initiated by TMPTA with three double bonds could capture not only semi-pinacol free radicals but also alkyl free radicals (near the surface of the particles) produced by the photoreduction of BP and emulsifier or other additives in the commercial NBR latex, and therefore the amounts of coupled SP could be greatly increased; and (2) the cross-linking reaction could result in the formation of a compact surface cross-linking layer, and, under a temperature of 85 °C, the above mentioned weak C–C bonds could be cleaved to generate surface-radicals which, in turn, could induce a surface grafting polymerization.

The existence of a TMPTA unit in the compact surface cross-linking layer was demonstrated by FTIR (Fig. 4) through an increase in the ratio of the peak height at 1718  $\text{cm}^{-1}$ , which corresponds to the C=O stretching of TMPTA, to the peak height at 2240  $\text{cm}^{-1}$ , which corresponds to the absorption of C≡N.

UV–vis spectra and  $^{13}\text{C}$  NMR analysis (Fig. 2) indicate the existence of semi-pinacol groups on the surface of the NBR latex. The absorption at 254 nm in the UV–vis spectrum corresponded to the absorption of the benzene ring in the semi-pinacol structure, while the resonance at 126 ppm could be ascribed to the carbon signals of the benzene units in the semi-pinacol structure. From Fig. 2(a), it can be clearly seen that for the untreated NBR latex, the 254 nm absorption was the lowest. The second lowest absorption was found for the reaction without TMPTA, having undergone irradiation for 90 min. In the reaction where TMPTA had been added, the absorption of semi-pinacol groups increased with irradiation time, indicating that more semi-pinacol groups were tethered on the NBR latex

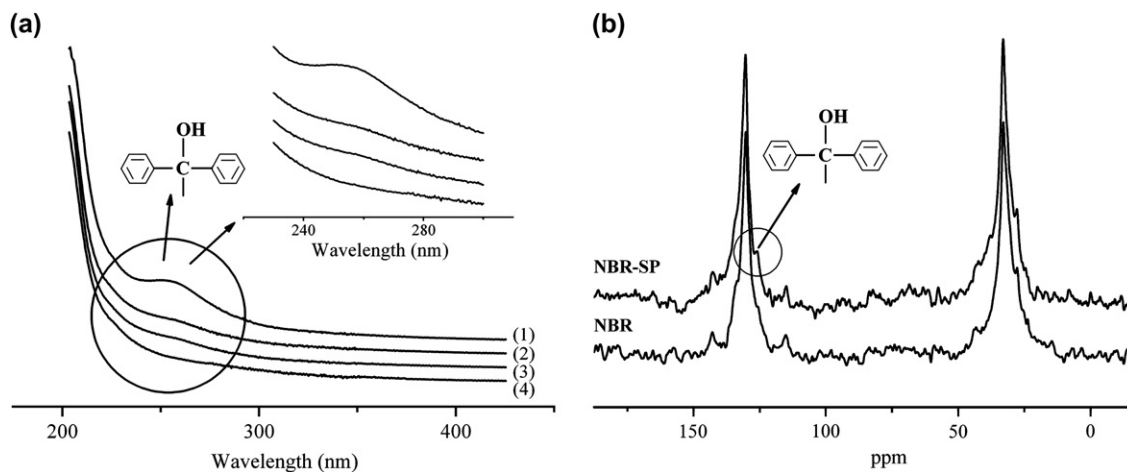


Fig. 2. (a) UV–vis spectra and (b)  $^{13}\text{C}$  NMR spectra of NBR coupled with semi-pinacol. Part (a) displays the different irradiation conditions used: (1) 90 min with TMPTA, (2) 30 min with TMPTA, (3) 90 min without TMPTA and (4) untreated NBR.

particles. These results confirmed the accelerating effect of TMPTA.

### 3.2. Grafting polymerization

The evolution of the St conversion, grafting yield and grafting efficiency with grafting polymerization time are shown in Fig. 3. Because the latex we used was a commercial product, some other impurity in NBR latex might induce polymerization. A control experiment used NBR latex without SP showed that no more than 4% St could be induced in control experiment. It is obvious that the conversion and grafting yield increased significantly during the first 80 min and then leveled off, while the grafting efficiency displayed a steep increase in the beginning after which it was almost constant.

For the polymerization conversion or rate, it was found, at first, that both the surface concentrations of SP and St were at high levels, and it was thus possible to maintain a high polymerization rate. While the grafting polymerization proceeded, the reaction rate gradually decreased. Compared with conventional grafting polymerization reactions, the relatively low end-conversion of monomer might be explained with the depletion of surface SP groups. Polymerization initiated with SP groups seems to be a living radical polymerization [33–35]. But, in our heterogeneous latex system, side termination reaction might consume the SP group on NBR surface. So, as can be seen in Fig. 3, polymerization terminated at a relatively low conversion of about 50%.

Moreover, the grafting yield increased from 13% to 37% as the polymerization time was extended from 30 min to 150 min. In fact, when increasing the ratio of St:NBR, to e.g., 70:30, the grafting yield could be increased even further, i.e. to 80%, 140%, etc.

Furthermore, a high grafting efficiency of approx. 90% is noted from Fig. 3. It is demonstrated that the amount of homopolymer could be dramatically reduced due to the very low initiation reactivity of the semi-pinacol radicals produced by decomposition of NBR–SP under 85 °C in the heterogeneous polymerization system.

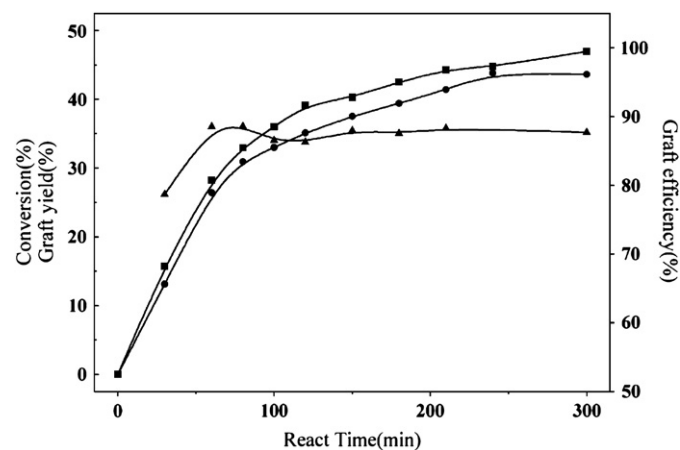


Fig. 3. Relationships between reaction time and monomer conversion (■), grafting yield (●) and grafting efficiency (▲). Conditions:  $C_{\text{NBR}} = 23.7$  wt%,  $C_{\text{St}} = 23.7$  wt%, at 85 °C.

After extraction with a solvent, the obtained core–shell particles were analyzed by FTIR spectroscopy, as shown in Fig. 4. Compared with the spectra of NBR (Fig. 4(a)) and pure PSt (Fig. 4(c)), it can be seen that besides the characteristic absorption band of the –CN group of NBR that appeared at  $2240\text{ cm}^{-1}$ , characteristic absorption bands of PSt were exhibited in the spectra of the NBR/PSt core–shell particles. The absorption band at around  $3023\text{ cm}^{-1}$  corresponded to the aromatic =C–H stretching of PSt while the band at around  $1597\text{ cm}^{-1}$  belonged to the C=C stretching of the aromatic PSt ring. The bands at around  $698\text{ cm}^{-1}$  and  $758\text{ cm}^{-1}$  corresponded to the aromatic =C–H stretching of PSt, and all these bands confirmed the formation of the grafted polymer.

### 3.3. Morphology of the core–shell particles

TEM micrographs (Fig. 5) display the morphology of the NBR/PSt core–shell particles with varying grafting yields of PSt. It is known that  $\text{OsO}_4$  can react with functional groups of unsaturated double bonds, as well as with hydroxyl and amine groups. The treatment with  $\text{OsO}_4$  thus provided a larger contrast for the TEM measurements. In the micrographs, a core–shell structure with a dark  $\text{OsO}_4$ -stained core and a grayish shell can be recognized very well. The NBR cores were darkened due to the unsaturated bonds reacting with  $\text{OsO}_4$ . It is clear in Fig. 5(b)–(d) that there is no secondary particle formed in grafting process. Laser-light scattering data also confirm that the distribution of particles' diameter did not change after grafting polymerization.

An interesting tendency from Fig. 5 was that the black region of the particles decreased in size while the gray region became larger with increasing grafting yield of St. Another interesting phenomenon was that the gray region broadened from the outside to the inside of the particles, finally, core–shell particles with black centers were formed. Based on the

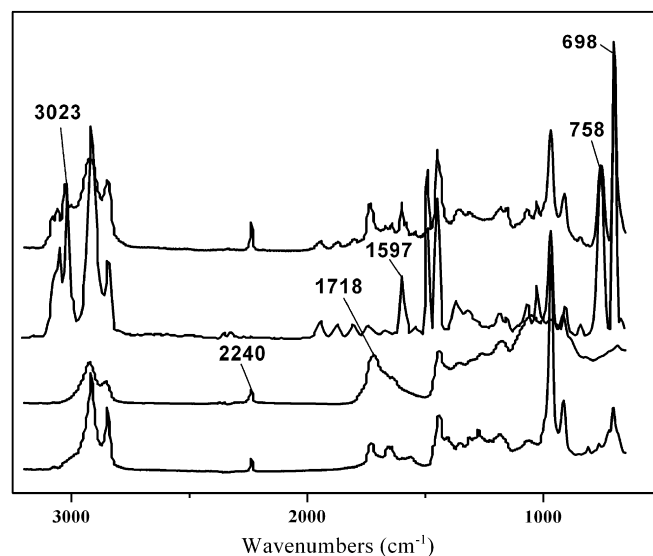


Fig. 4. FTIR spectra of (a) untreated NBR, (b) NBR–SP irradiated for 90 min, (c) pure PSt and (d) NBR/PSt core–shell particles.



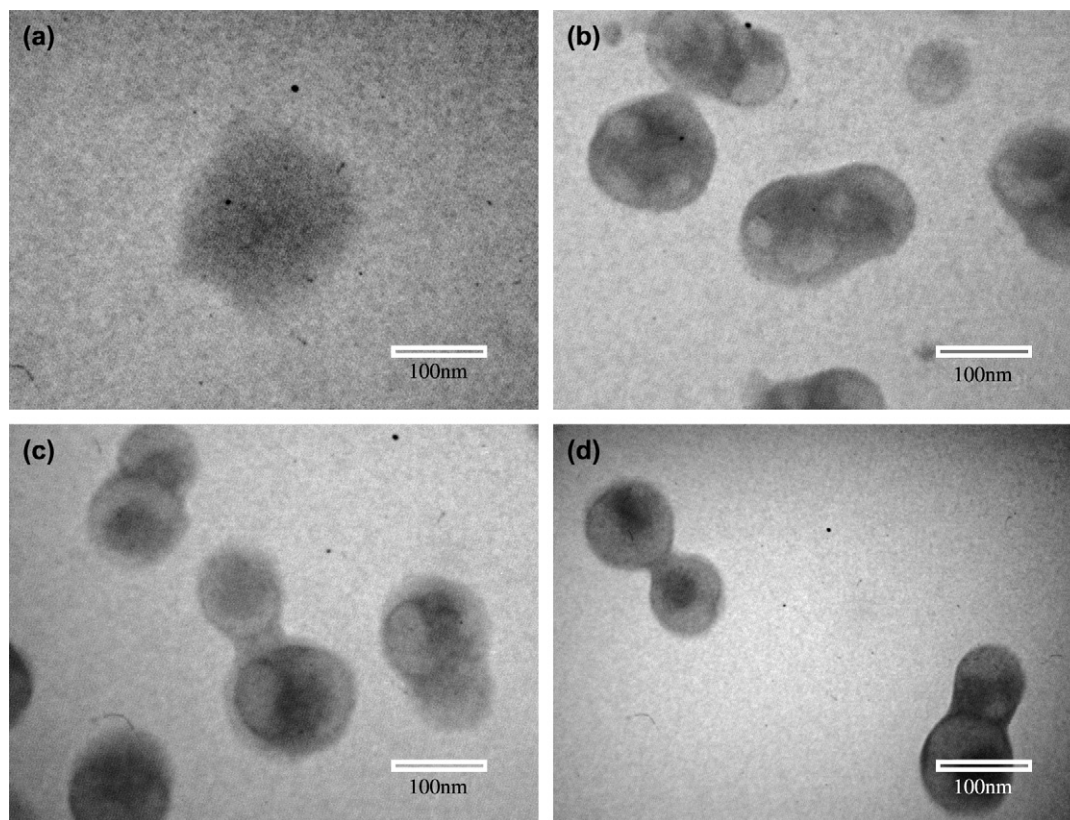


Fig. 5. TEM micrographs of NBR/PSt particles with varying grafting yield: scale bar = 100 nm; (a) GY = 0%, (b) GY = 9.8%, (c) GY = 46% and (d) GY = 136%. Conditions:  $C_{\text{NBR}} = 4.3 \text{ wt\%}$ ,  $C_{\text{St}} = 10 \text{ wt\%}$ , at  $85 \text{ }^\circ\text{C}$ .

results above, a grafting model could be described according to the following: during heating, the grafting polymerization started from the surface of the NBR–SP, and then developed towards the particle centers due to St being swollen in the NBR particle. During polymerization, the double bonds in the NBR backbone took part in the copolymerization with St, not only resulting in cross-linking but also producing a non-stained layer due to the disappearance of double bonds.

Moreover, from the TEM micrographs (Fig. 5(b)–(d)), the particle sizes seemed to become somewhat smaller than those of the primary NBR particles. In order to clear up this phenomenon, the size of the NBR/PSt core–shell particles with varying grafting yields in diluted latex was determined by laser-light scattering measurement, and the results are listed in

Table 1  
The diameters of NBR/PSt particles with varying grafting yield as measured by TEM and laser-light scattering

Reaction time (min)	Grafting yield (%)	Particle size in TEM <sup>a</sup> (nm)	Thickness of grafted layer <sup>a</sup> (nm)	Core size in TEM <sup>a</sup> (nm)	Particle size obtained by laser-light scattering (nm)
0	0	180	0	180	101
60	9.8	110	12.5	85	103
100	46	112	20.5	71	103
150	84	–	–	–	107
210	136	95.5	22.4	50.6	118
300	142	–	–	–	113

<sup>a</sup> Measured directly from the TEM images.

Table 1. Other relevant parameters such as the reaction time, the grafting yield and particle sizes obtained from the TEM micrographs in Fig. 5 are also listed in Table 1.

According to the data in Table 1, the diameter of the core–shell particles did not display an obvious increase, merely a few nanometers, despite the large increase in yield with polymerization time. This phenomenon might be understandable when considering that the growth of the grafted polymer chain occurred from the surface of particle towards the center, which could increase the density of the particles, whilst maintaining the size of the particles almost constant. On the other hand, the diameters of dried core–shell particles obtained by TEM were very different from the above results. For primary particles or particles with a low grafting yield, the values were larger than for the former ones, whereas for particles with a high grafting yield, the values were smaller. This phenomenon might be attributed to the deformation and collapse of soft NBR particles so that they became disk-shaped during vacuum drying. This tendency towards deformation and collapse may be mitigated by attaching a hard layer of PSt, which should give rise to smaller particles.

### 3.4. Preparation of composite core–shell particles

Re-grafting of hydrophilic AM and amphiphilic NVP monomers on the NBR/PSt core–shell particles (GY = 42%) was performed by adding a sequential monomer. With

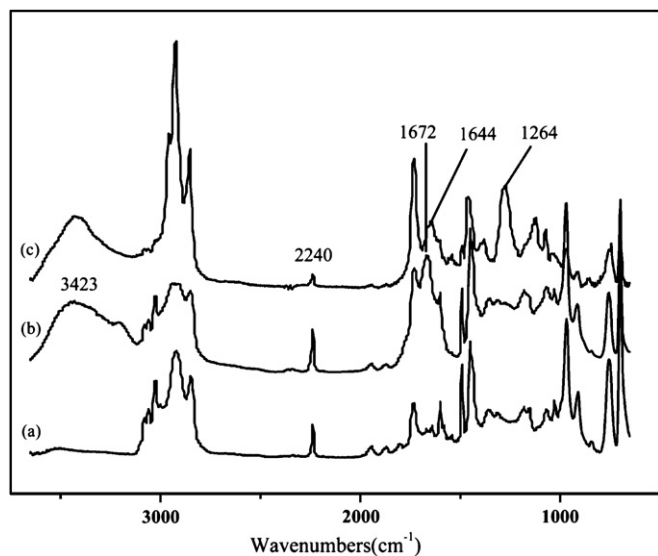


Fig. 6. FTIR spectra of (a) NBR/PS, (b) NBR-g-PS/PAm and (c) NBR-g-PS/PVP.

the grafting of PAm or PVP, the latex became more stable. It would not be precipitated with the 2% calcium chloride solution. The grafting yield to NBR increased from 42% to 61% for NBR-g-PS/PAm whereas it was 54% for NBR-g-PS/PVP.

IR spectra (Fig. 6) demonstrated the successful grafting of PAm (or PVP) onto the NBR/PS particle surfaces. The strong characteristic absorption bands at  $1672\text{ cm}^{-1}$  and  $3423\text{ cm}^{-1}$  were ascribed to the vibration of C=O and NH, respectively. The absorption visible at  $1644\text{ cm}^{-1}$  was attributed to the ring vibration of the pyrrolidone groups of PVP and the peak at  $1264\text{ cm}^{-1}$  corresponded to the N–C vibration of the pyrrolidone group.

Fig. 7 shows the TEM micrographs of various core–shell particles. Core–shell structures with a dark core stained with  $\text{OsO}_4$  and a light shell can be readily recognized. The gray circle around PS represented the PAm shell formed in the second grafting polymerization, and correspondingly, the gray circle in Fig. 7(c) represented the PVP shell. From the images of these core–shell particles, it was clear that the particle size of the NBR-g-PS/PVP core–shell structure was much bigger than the others. This may be explained by the swelling. Because of the amphiphilic property of NVP, some of the NVP could dissolve inside NBR/PS particles during the grafting polymerization. As a result, after polymerization, the PVP chain within the particles would absorb water from the outer environment, causing the particle to swell into a bigger one. This is consistent with the laser-light scattering measurements, which indicated that the particle size of the NBR/PS core–shell structure increased from 109 nm to 127 nm as it became NBR-g-PS/PAm. The NBR-g-PS/PVP core–shell structure obtained an even greater diameter of 186 nm.

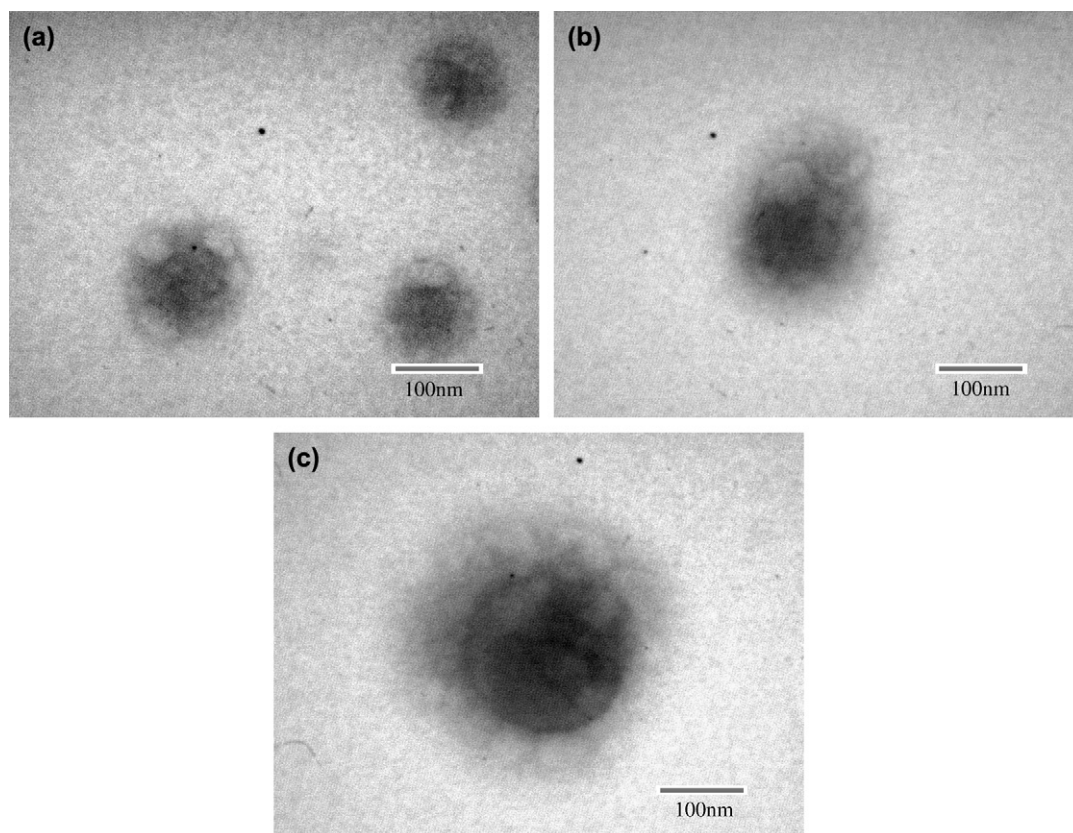


Fig. 7. TEM micrographs of (a) NBR/PS, (b) NBR-g-PS/PAm and (c) NBR-g-PS/PVP. Conditions:  $C_{\text{NBR/PS}} = 5.7\text{ wt\%}$  (grafted for 2 h GY = 42%),  $C_{\text{AM}} = 7.1\text{ wt\%}$  in (b);  $C_{\text{NVP}} = 7.1\text{ wt\%}$  in (c), grafted at  $85\text{ }^\circ\text{C}$  for 3 h.

#### 4. Conclusion

In conclusion, the composite core–shell particles based on NBR latex were successfully synthesized through a two-step method. In the first step, by taking advantage of a UV-screening effect and introducing a multi-functional monomer, a surface-compact cross-linking NBR–SP rubber particle was obtained. In the second step, through heating, the cleavage of weak C–C bonds between the SP groups and the surface chains of the NBR particle resulted in the generation of grafted polymers with a high grafting efficiency. Chain propagation started from the surface and grew inwards to the particle center. Through addition of a second hydrophilic or amphiphilic monomer, a composite core–shell particle could be prepared.

#### Acknowledgements

We gratefully acknowledge financial support from the National Natural Science Foundation of China (NSFC), major project (No. 50433040, No. 20374004) and the Polymer Chemistry and Physics, BMEC (No. XK 100100433, No. XK 100100540).

#### References

- [1] Marinakos SM, Brousseau III LC, Jones A, Feldheim DL. *Chem Mater* 1998;10:1214–9.
- [2] Quaroni L, Chumanov G. *J Am Chem Soc* 1999;121:10642–3.
- [3] Xiong Y, Chen GS, Guo SY. *J Appl Polym Sci* 2006;102:1084–91.
- [4] Chen JP, Su DR. *Biotechnol Prog* 2001;17:369–75.
- [5] Sparnacci K, Laus M, Tondelli L, Magnani L, Bernardi C. *Macromol Chem Phys* 2002;203:1364–9.
- [6] Pusch J, van Herk AM. *Macromolecules* 2005;38:6909–14.
- [7] Dimonie V, Elaasser MS, Klein A, Vanderhoff JW. *J Polym Sci Part A Polym Chem* 1984;22:2197–215.
- [8] Landfester K, Rothe R, Antonietti M. *Macromolecules* 2002;35:1658–62.
- [9] Li P, Zhu J, Sunintaboon P, Harris FW. *Langmuir* 2002;18:8641–6.
- [10] Fleming MS, Mandal TK, Walt DR. *Chem Mater* 2001;13:2210–6.
- [11] Schneider G, Decher G. *Nano Lett* 2004;4:1833–9.
- [12] Jang J, Ha H. *Chem Mater* 2003;15:2109–11.
- [13] Shenoy DB, Antipov AA, Sukhorukov GB, Mohwald H. *Biomacromolecules* 2003;4:265–72.
- [14] Li WH, Stover HDH. *Macromolecules* 2000;33:4354–60.
- [15] O'Reilly RK, Joralemon MJ, Hawker CJ, Woolley KL. *J Polym Sci Part A Polym Chem* 2006;44:5203–17.
- [16] Husemann M, Mecerreyes D, Hawker CJ, Hedrick JL, Shah R, Abbott NL. *Angew Chem Int Ed* 1999;38:647–9.
- [17] Prucker O, Rühle J. *Adv Mater* 1998;10:1073–7.
- [18] Quirk RP, Mathers RT, Cregger T, Foster MD. *Macromolecules* 2002;35:9964–74.
- [19] Zhao B, Brittain WJ. *Macromolecules* 2000;33:342–8.
- [20] Kong X, Kawai T, Abe J, Iyoda T. *Macromolecules* 2001;34:1837–44.
- [21] Husseman M, Malmstrom EE, McNamara M, Mate M, Mecerreyes D, Benoit DG, et al. *Macromolecules* 1999;32:1424–31.
- [22] Yu WH, Kang ET, Neoh KG. *Langmuir* 2005;21:450–6.
- [23] de Boer B, Simon HK, Werts MPL, van der Vegte EW, Hadziioannou G. *Macromolecules* 2000;33:349–56.
- [24] Bergbreiter DE, Srinivas B, Gray HN. *Macromolecules* 1993;26:3245–6.
- [25] Guo X, Weiss A, Ballauff M. *Macromolecules* 1999;32:6043–6.
- [26] Fulghum TM, Patton DL, Advincula RC. *Langmuir* 2006;22:8397–402.
- [27] Zheng G, Stover HDH. *Macromolecules* 2002;35:6828–34.
- [28] Kitano H, Anraku Y, Shinohara H. *Biomacromolecules* 2006;7:1065–71.
- [29] Smulders W, Monteiro MJ. *Macromolecules* 2004;37:4474–83.
- [30] Yang Q, Hu MX, Dai ZW, Tian J, Xu ZK. *Langmuir* 2006;22:9345–9.
- [31] Rohr T, Hilder EF, Donovan JJ, Svec F, Frechet JMJ. *Macromolecules* 2003;36:1677–84.
- [32] Rånby B, Yang WT, Tretinnikov O. *Nucl Instrum Methods Phys Res B* 1999;151:301–5.
- [33] Yang WT, Rånby B. *Macromolecules* 1996;29:3308–10.
- [34] Ma H, Davis RH, Bowman CN. *Macromolecules* 2000;33:331–5.
- [35] Yamamoto K, Kyouzuka S, Shimada S. *Macromolecules* 2004;37:86–91.
- [36] Guo X, Ballauff M. *Langmuir* 2000;16:8719–26.
- [37] Liu LY, Yang WT. *J Polym Sci Part A Polym Chem* 2004;42:846–52.
- [38] Ratnam CT, Nasir M, Baharin A, Zaman K. *J Appl Polym Sci* 2001;81:1926–35.
- [39] Majumder PS, Bhowmick AK. *Radiat Phys Chem* 1999;53:63–78.
- [40] Vijayabaskar V, Bhowmick AK. *J Appl Polym Sci* 2005;95:435–47.